

Beam-ion transport dependence on Magnetic Perturbations spectrum and plasma helicity in the ASDEX Upgrade tokamak

L. Sanchis¹, M. Garcia-Munoz², E. Viezzer², A. Snicker¹, J. Gonzalez-Martin²,
J. Galdon-Quiroga³, L. Chen⁴, F. Zonca⁵, D. Zarzoso⁶, W. Suttrop³,
M. Willensdorfer³ and the AUG[†] team

¹ *Aalto University, Espoo, Finland*; ² *University of Sevilla, Sevilla, Spain*; ³ *Max Planck IPP, Garching, Germany*; ⁴ *IFTS, Zhejiang University, Hangzhou, China*; ⁵ *ENEA, Frascati, Italy*;
⁶ *Aix-Marseille Université, CNRS, PIIM, UMR 7345, Marseille, France*

Introduction

Externally applied magnetic perturbations (MPs) are commonly used in tokamaks to control ELM instabilities [1]. However, the associated symmetry breaking of the magnetic fields can degrade the fast-ion confinement, thus possibly endangering the integrity of future devices [2]. Previous analysis have shown that, in the presence of MPs, beam-ions are affected by a resonant transport located at plasma edge. It was also found numerically that the poloidal spectra of the perturbation can be optimised to minimise the fast-ion confinement degradation while still mitigating ELMs [3]. Apart from the poloidal spectrum dependence, experiments in ASDEX Upgrade (AUG) have also shown that the amplitude of the measured beam-ion losses depend on the MP toroidal spectrum and the magnetic background helicity (q_{95}) [4].

In AUG, the externally applied MPs are generated by two rows of 8 coils located above and below the midplane. By changing the current flowing through the individual coils, it is possible to change the toroidal and poloidal mode numbers of the perturbation. The toroidal symmetry of the current waveform sets the toroidal spectrum while a variation of the phase between the upper and lower set of coils can modify the poloidal spectrum. The symmetry breaking caused by the 3D fields induces a variation in the particle toroidal canonical momentum (δP_ϕ). This change is associated with a radial drift of the particle where a positive variation of δP_ϕ leads to an inwards transport while a negative variation implies an outwards transport.

The aim of this study is to analyse the beam-ion transport in terms of the magnetic shear q_{95} and the toroidal spectrum by means of experimental data and full-orbit simulations using the ASCOT code. Additionally, the identification of the transport mechanism responsible for the beam-ion losses was done in the framework of linear and nonlinear resonant transport theory [5].

Impact of the magnetic field helicity on the edge resonant transport layer (ERTL)

The analysis of the effect of q_{95} on the beam-ion transport induced by MPs was motivated by the results of two experiments in AUG. Discharges AUG#28059 and AUG#28061 had similar

plasma shapes and the same MP configuration was applied. The MP was generated by a $I = 1$ kA current and had an $n = 2$ toroidal symmetry with a phase shift of $\Delta\phi_{UL} = 180^\circ$ (figure 1 a)). The only difference between the shots was the q_{95} value, which was $q_{95} = 3.8$ for AUG#28061 and $q_{95} = 5.5$ for AUG#28059 (figure 1 b)).

In both cases, the beam-ion losses were analysed using the fast-ion loss detector (FILD1). Figure 1 c) shows the beam-ion loss signal for the case with high q_{95} (red) and low q_{95} (blue) indicating that the beam-ion losses are increased by a factor of 6 in the low q_{95} case. One of the contributions to this difference in the beam-ion losses can be explained in terms of resonant transport. By computing the $\langle\delta P_\phi\rangle$ in each case, it is possible to localise and characterise the beam-ion transport. In figure 2, $\langle\delta P_\phi\rangle$ is computed in vacuum approach as a function of the beam-ion initial energy and radial location starting at the midplane with pitch $\lambda = v_{\parallel}/v = -0.5$. For AUG#28061, the transport is localised within 5 cm around the separatrix and the sign on the $\langle\delta P_\phi\rangle$ indicates a dominant outward transport. In the AUG#28059 case, the sign of the transport is similar but the transport layer has shifted inwards (figure 2 b)). This change on the transport radial location has a double effect, first it shifts the maximum outward transport away from beam ions born at the edge, which are more susceptible to escape confinement. The second effect is a decrease in the intensity of the transport as the resonant condition is moved further from the MP coils. Additionally, a third case with the same plasma shape and higher helicity ($q_{95} = 6.1$) given by AUG#33145, was simulated applying the same MP configuration. Figure 2 c) shows the $q_{95} = 6.1$ case, where the transport layer presents a deeper inwards shift. In figure 2 c), the δP_ϕ profiles are plotted for the three cases as a function of the initial radial location at energy $E = 45$ keV showing more clearly the inward shift and intensity decrease of the ERTL as the q_{95} is increased.

Using the $\langle\delta P_\phi\rangle$ representation, it is also possible to identify the the resonant condition responsible for the ion transport. The $\langle\delta P_\phi\rangle$ patterns have been analysed by overplotting the $\omega_{pol}/\bar{\omega}_{tor}$ coefficients where ω_{pol} and $\bar{\omega}_{tor}$ are the beam-ion bounce and precession frequencies. The general resonant condition for trapped ions is given by [5]

$$\frac{\omega_b}{\bar{\omega}_d} = \frac{n(l+1)}{p(l+1) + p'} \quad (1)$$

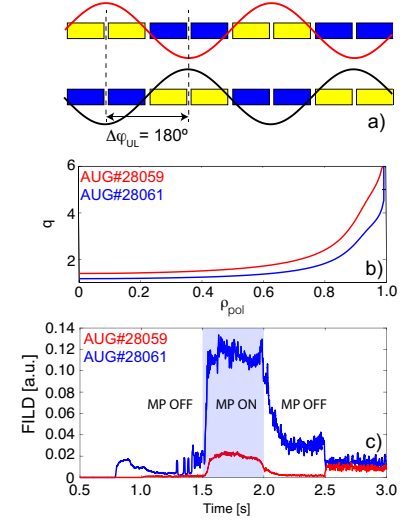


Figure 1: a) Coil configuration corresponding to $\Delta\phi_{UL} = 180^\circ$. b) Safety factor profile for shots AUG#28061 (blue) and AUG#28059 (red). c) Measured beam-ion losses.

where n is the toroidal mode, l is the nonlinear harmonic, p is the primary bounce harmonic, and p' is the nonlinear bounce harmonic. In the three cases analysed, the ion transport is caused by the $\omega_{pol}/\bar{\omega}_{tor} = 2$ condition, corresponding to the linear ($l = 0$) resonance $n = 2$, $p = 1$.

Impact of a mixed toroidal spectra on the ERTL

The analysis of $\langle \delta P_\phi \rangle$ was applied to study the effects of the MP toroidal spectrum on the beam-ion transport. In particular, an MP configuration with a mixed toroidal spectrum was analysed to evaluate the impact that the combination of $n = 2$ and $n = 4$ toroidal modes has on the resonant structures in the particle velocity-space. Each component was produced by a $I = 0.5$ kA current resulting in a maximum of 1 kA on some coils. In the AUG#36523 discharge, the $n = 4$ component was fixed at $\Delta\phi_{UL(n=4)} = 180^\circ$ while the phase shift of the $n=2$ was continuously varied in time. In order to analyse the beam-ion transport, figure 3 shows $\langle \delta P_\phi \rangle$ in vacuum approach as a function of the ion initial energy and radial location launched from the midplane with $\lambda = -0.5$. In this time point, $t = 2.5$ s, the phase shift is $\Delta\phi_{UL(n=2)} = \Delta\phi_{UL(n=4)} = 180^\circ$ for both components. The effect of each component was studied separately by isolating only one toroidal harmonic and then comparing the transport with the case containing the full toroidal spectrum.

Similar to the previous section, the resonant identification was done by comparing the $\langle \delta P_\phi \rangle$ patterns with the $\omega_{pol}/\bar{\omega}_{tor}$ coefficients. Figure 3 a) shows the radial transport through $\langle \delta P_\phi \rangle$ considering only the $n = 2$ mode number. In this case, the main resonance responsible for the beam-ion transport is defined by $\omega_{pol}/\bar{\omega}_{tor} = 2$, which corresponds to the linear condition associated to $n = 2$, set by the external perturbation, and $p = 1$. In figure 3 b) the isolated $n = 4$ was considered, revealing that transport is caused by the resonant conditions $\omega_{pol}/\bar{\omega}_{tor} = 4, 2, 1.33, 1.20$. The $\omega_{pol}/\bar{\omega}_{tor} = 4, 2, 1.33$ correspond to linear resonances associated to $n = 4$ and $p = 1, 2, 3$, which are the dominant contribution to the ion transport. The $\omega_{pol}/\bar{\omega}_{tor} = 1.20$ structure is a nonlinear resonance given by $n = 4, l = 2, p = 3, p' = 1$, but the effect of this transport is very limited as it is located outside the separatrix. Figure 3 c) shows that the resonances associated to each toroidal mode number are present in the case including the full toroidal spectrum, leading to a resonance overlap that can either enhance or reduce the particle transport depending on the perturbation $\Delta\phi_{UL}$ of each toroidal component.

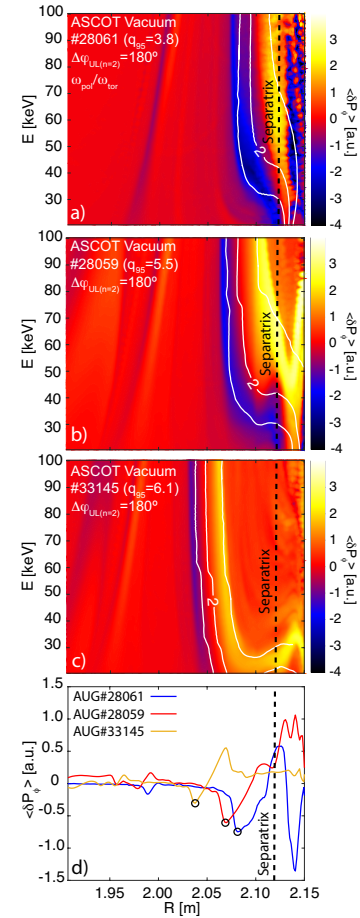


Figure 2: a)-c) $\langle \delta P_\phi \rangle$ for different $\Delta\phi_{UL}$. The white lines indicate the geometrical resonances. d) $\langle \delta P_\phi \rangle$ profile for a fixed energy $E=45$ keV.

In the combined transport shown in figure 2 c), the effect of the superposition of the toroidal spectra is to reduce the outward transport in the region inside the separatrix. In figure 3 d), $\langle \delta P_\phi \rangle$ is presented for a $\Delta\varphi_{UL(n=2)} = 90^\circ$ coil configuration showing an outward ion transport that is enhanced when combined with the $n = 4$ component (figure 3 e)).

Summary and conclusions

The beam-ion resonant transport in the presence of externally applied magnetic perturbations was characterised in terms of the MP spectrum and the magnetic field q_{95} using experimental data and full-orbit simulations. Through the variation of the particle P_ϕ , it was observed that q_{95} affects the beam-ion transport due to a shift of the resonant transport layer. Higher q_{95} leads to an inward shift that contributes to reducing the beam-losses by displacing the transport layer from the beam ions born at the edge and decreasing the transport intensity as the MP δB amplitude is weaker towards the plasma core. The inclusion of a mixed toroidal spectrum leads to a superposition of the resonances associated to each toroidal mode. This makes it possible to control the intensity of the transport by combining different toroidal spectra and $\Delta\varphi$ to minimise the outward transport of beam ions while still mitigating the ELMs.

Acknowledgments: This work has been carried out within the framework of the EUROfusion Consortium and has received funding from the Euratom research and training programme 2014-2018 and 2019-2020 under grant agreement No 633053. The views and opinions expressed herein do not necessarily reflect those of the European Commission.

References

- [1] T. E. Evans et al, Nature Physics **2**, 419 (2006)
 - [2] M. Garcia-Munoz et al, Plasma Physics and Controlled Fusion **55**, 124014 (2013)
 - [3] L. Sanchís et al, Nuclear Fusion **61**, 046006 (2021)
 - [4] M. Garcia-Munoz et al, Plasma Physics Controlled Fusion **55**, 124014 (2013)
 - [5] F. Zonca et al, Journal of Plasma Physics **81**, 495810515 (2015)
- † See author list of H. Meyer et al., Nuclear Fusion **59**, 112014 (2019)

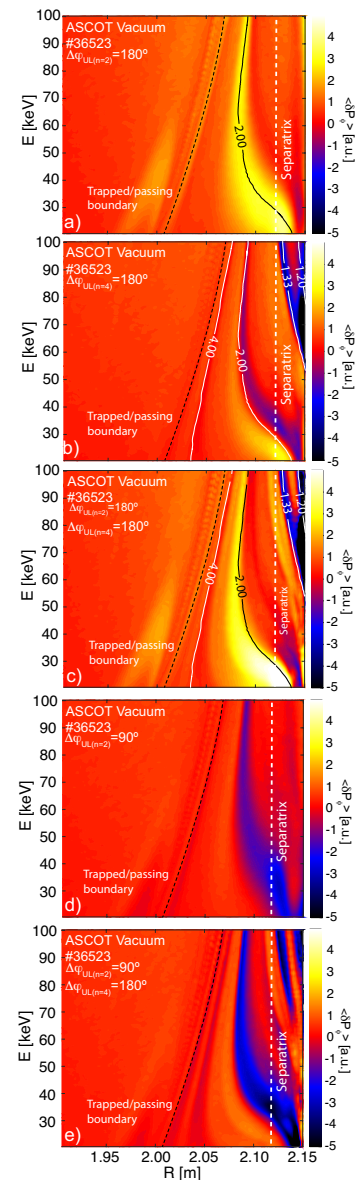


Figure 3: $\langle \delta P_\phi \rangle$ for $\Delta\varphi_{UL(n=2)} = 180^\circ$ with a) $n=2$, b) $n=4$ and c) all n . $\langle \delta P_\phi \rangle$ for $\Delta\varphi_{UL(n=2)} = 90^\circ$ with d) $n=2$ and e) all n .